Trees
https://doi.org/10.1007/s00468-024-02499-5

ORIGINAL ARTICLE

Xylem safety in relation to the stringency of plant water potential regulation of European beech, Norway spruce, and Douglas-fir trees during severe drought

Katja Schumann[1] · Bernhard Schuldt[1,2] · Miriam Fischer[1] · Christian Ammer[3] · Christoph Leuschner[1]

Received: 10 June 2023 / Accepted: 9 February 2024

Abstract

Key message **Norway spruce operates with larger hydraulic safety margins (HSM) than beech and Douglas-fir despite the known drought sensitivity of spruce, questioning a pivotal role of HSM in drought tolerance.**

Abstract The exceptional 2018/2019 drought exposed Central Europe's forests to severe stress, highlighting the need to better understand stomatal regulation strategies and their relationship to xylem safety under extreme drought. We studied diurnal, seasonal, and inter-annual variation in stomatal conductance (g_s) and leaf water potential (Ψ_{Leaf}) in co-occurring European beech (*F. sylvatica*), Norway spruce (*P. abies*), and Douglas-fir (*P. menziesii*) trees in the two summers and related them to hydraulic traits characterizing drought resistance. In 2018, *F. sylvatica* exhibited a continuous Ψ_{Leaf} decline from June to September, as is characteristic for an anisohydric strategy, while *P. abies* closed stomata early and reached the least negative Ψ_{Leaf}-values at the end of summer. *P. menziesii* showed low Ψ_{Leaf}-values close to P_{12} (the xylem pressure at onset of embolism) already in July. Both conifers closed stomata when approaching P_{12} and maintained low g_s-levels throughout summer, indicative for isohydric regulation. In 2019, all three species showed a linear decline in Ψ_{Leaf}, but *F. sylvatica* crossed P_{12} in contrast to the conifers. The three species exhibited similar water potentials at turgor loss point (− 2.44 to − 2.51 MPa) and branch P_{50} (xylem pressure at 50% loss of hydraulic conductance; − 3.3 to − 3.8 MPa). Yet, *F. sylvatica* and *P. menziesii* operated with smaller hydraulic safety margins (HSM means: 0.79 and 0.77 MPa) than *P. abies* (1.28 MPa). *F. sylvatica* reduced leaf size and specific leaf area in 2019 and increased Huber value. Our species comparison during extreme drought contradicts the general assumption that conifers operate with larger HSMs than angiosperm trees. Contrary to expectation, *P. abies* appeared as hydraulically less vulnerable than Douglas-fir.

Keywords Embolism resistance · Iso/anisohydric · Hydraulic safety margin · Leaf water potential · Stomatal regulation · Turgor loss point · Vulnerability curve

Introduction

The exceptional summer drought episode of 2018/2019 has exposed many European forests to extreme stress caused by the joint action of atmospheric and edaphic drought and heat (Obladen et al. 2021; Walthert et al. 2021; Frei et al. 2022). 2018 was the warmest year in Germany since the start of weather recording in 1881, with mean annual temperature (10.4 °C) being 2.2 °C above the long-term mean (1961–1990), and annual precipitation (435 mm) reaching only 58% of the long-term mean (747 mm). In correspondence, vapor pressure deficit reached record highs, thus enhancing atmospheric drought stress (Williams et al. 2013), while the deficit in the climatic water balance was the second largest ever recorded in the region (Schuldt et al. 2020). This

Communicated by Varone.

✉ Christoph Leuschner
cleusch@gwdg.de

[1] Plant Ecology, University of Goettingen, Untere Karspüle 2, 37073 Göttingen, Germany

[2] Chair of Forest Botany, Institute of Forest Botany and Forest Zoology, Technische Universität Dresden, Pienner Str. 7, 01737 Tharandt, Germany

[3] Silviculture and Forest Ecology of the Temperate Zones, University of Goettingen, Büsgenweg 1, 37077 Göttingen, Germany

Published online: 23 March 2024

drought event apparently was the most extreme in the last 2100 years in Central Europe (Büntgen et al. 2021).

In addition to climate warming, some Central European regions have experienced reductions in mid-summer precipitation in recent decades, which increases climatic drought in the physiologically most important season (Trnka et al. 2015; Bat-Enerel et al. 2022). As a consequence, widespread canopy dieback and tree mortality have recently been reported in various Central European regions (Schuldt et al. 2020; Senf et al. 2020; Braun et al. 2021; Thonfeld et al. 2022) with especially Norway spruce (*Picea abies* Karst.), but also European beech (*Fagus sylvatica* L.), Scots pine (*Pinus sylvestris* L.), *Quercus* species, and Douglas-fir (*Pseudotsuga menziesii* (Mirb.) Franco) being affected. The infestation of weakened trees with pest organisms often has accelerated stand decline. Climate models predict that such extreme hot droughts likely will increase in frequency and severity in Europe with advancing climate warming (Fischer and Schär 2008; Spinoni et al. 2018). This has raised concern among forest scientists and foresters about the suitability of Central Europe's main timber species for silviculture in a future warmer climate.

Norway spruce, European beech, and Douglas-fir are the economically most important timber species of Central Europe, together with Scots pine and two oak species (*Quercus petraea* (Matt.) Liebl. and *Q. robur* L.) (Thünen Institute 2015). All three species were more or less affected by the hot droughts of the recent past, but their drought sensitivity and drought response strategies likely are dissimilar. *F. sylvatica* is the dominant tree species of Central Europe's natural forests, which would cover about two thirds of Germany's forest area in the absence of human influence (Bohn et al. 2003; Leuschner and Ellenberg 2017). Despite its competitiveness, *F. sylvatica* has been assessed as relatively sensitive to drought and heat (Gessler et al. 2004; Leuschner 2020; Schuldt et al. 2020; Walthert et al. 2021; Arend et al. 2022; Leuschner et al. 2023). *P. abies* is native to Central Europe's higher mountains and is widespread in the boreal zone, but has been planted widely in lower montane and lowland regions outside of its natural range, since it is a fast-growing species whose wood is demanded for multiple purposes. Despite widespread damage by droughts, subsequent insect attack and windbreak in recent decades, it is still the economically most important timber species in Germany and other Central European countries, even though its percentage has decreased constantly in the past three decades (Thünen Institute 2015; Leuschner and Ellenberg 2017). Yet, numerous studies evidence the drought sensitivity of this species (Tumajer et al. 2017; Krejza et al. 2021). The North American conifer *P. menziesii* has been planted in Central Europe since the nineteenth century and covers about 2% of the recent forest area in Germany (Thünen Institute 2015) and 3% in France (Zeller et al. 2019). It is favored by European foresters as a possible replacement for *P. abies* in production forests due to its high productivity, excellent wood properties and assumed high drought resistance (Spiecker et al. 2019). From published work on subjective assessments of the drought resistance of the three species, a principal ranking of the species in the sequence *P. abies* < *F. sylvatica* < *P. menziesii* seems to emerge (Niinemets and Valladares 2006).

One of the traits determining a tree species' drought vulnerability is the embolism resistance of its xylem. The P_{50}- and P_{88}-values, i.e., the xylem pressures at which 50% or 88% of hydraulic conductivity is lost, have widely been used for comparing tree species' sensitivity to drought (Maherali et al. 2004; Choat et al. 2012; Lobo et al. 2017). It is thought that many woody species operate relatively close to their hydraulic safety margin (HSM), where minimum leaf water potential meets the critical value of embolism onset in the xylem. Yet, conifers tend to die at lower PLC (percentage loss of conductance) values than angiosperms (Urli et al. 2013), which may have led in many conifers to the evolution of larger HSMs than in angiosperm trees (Choat et al. 2012; Carnicer et al. 2013). Recorded P_{50} (and P_{88}) values in mature trees of the three species here considered vary with hydrological site conditions, with more negative values often recorded at drier sites (Schuldt et al. 2016; Tomasella et al. 2017). According to the literature (Cochard 1992; Hacke and Sauter 1995; Sperry and Ikeda 1997; Piñol and Sala 2000; Maherali et al. 2004; Wortemann et al. 2011; Schuldt et al. 2016; Weithmann et al. 2022b), *F. sylvatica* shows the highest P_{50}-values (ranging from − 2.8 to − 3.8 MPa), *P. menziesii* the lowest (from − 3.7 to − 5.5 MPa), and *P. abies* intermediate values (from − 3.5 to − 4.0 MPa). This would suggest the greatest embolism resistance in *P. menziesii* and the lowest in *F. sylvatica*, partly contradicting the sequence of drought resistances given for the three species in Niinemets and Valladares (2006). Less is known about the three species' HSMs.

How plants regulate water potential variation determines their response to drought, notably the capacity to maintain carbon assimilation under water deficits. With respect to the ability to regulate leaf water potential (Ψ_{Leaf}), plants have frequently been categorized according to their degree of isohydry. While isohydric species maintain leaf water potential fairly constant, anisohydric species tolerate greater drops in Ψ_{Leaf} (Klein 2014). *F. sylvatica* has been characterized as markedly anisohydric (Leuschner et al. 2021), allowing for large diurnal and seasonal Ψ_{Leaf} variation, while *P. abies* seems to pursue a more isohydric strategy (Lyr et al. 1992; Leo et al. 2014; Zweifel et al. 2009). For *P. menziesii*, both isohydric and anisohydric regulation has been reported for different provenances and growth conditions (Anekonda et al. 2002; Warren et al. 2004; Link et al. 2014; Jansen 2017; Kerhoulas et al. 2020).

A direct comparison of the three species with respect to traits determining drought vulnerability is lacking so far, especially for mature trees growing under similar environmental conditions. It, thus, remains unclear how the three species are to be ranked with respect to their drought vulnerability. Yet, a comparative assessment of the three species' drought resistance is urgently needed, given their importance as timber species in Central Europe and the threat posed by global warming.

Conifer and angiosperm trees differ in their wood anatomy, with the latter developing more complex woody tissues with tracheae and higher parenchyma fraction in comparison to the simpler tracheid-dominated conifer wood. The tracheids of conifer xylem are usually smaller than angiosperm vessels and often more resistant to embolism formation (Tyree and Zimmermann 2002). There is some evidence that these differences in wood anatomy also relate to stomatal regulation stringency and patterns of Ψ_{Leaf} variation, as it appears that isohydric regulation is more frequent in temperate and boreal conifers, while angiosperm trees seem to display more often anisohydric regulation (Carnicer et al. 2013; Martinez-Sancho et al. 2017; Blackman et al. 2019). Yet, isohydric angiosperms and anisohydric conifers do also exist (Voelker et al. 2018; Leuschner et al. 2019). It has been postulated that many conifers lack the capacity to repair drought-induced embolism due to a low wood parenchyma fraction and, thus, lower non-structural carbohydrate levels in their stem wood, which could explain the need for greater HSM (Johnson et al. 2012; Carnicer et al. 2013).

Here, we present the results of a comparative study of hydraulic and leaf water status traits in *F. sylvatica*, *P. abies,* and *P. menziesii* trees under exposure to severe natural drought, which might help defining hydrological thresholds of these three important timber species. Our study in the exceptionally dry and hot summers of 2018 and 2019, enhanced by low precipitation in winter 2018/2019, is a welcome case study of the vulnerability of these three important Central European timber species to climatic extremes, as they are predicted to occur more frequently in future with climate warming (Fischer and Schär 2008; Meinke et al. 2010; Spinoni et al. 2018). We measured diurnal, seasonal, and inter-annual variation in stomatal conductance and leaf water potential, established branch xylem vulnerability curves (P_{12}-, P_{50}-, P_{88}-values), and measured leaf tissue turgor loss point (π_{tlp}), and leaf and branch morphological traits [leaf size, specific leaf area (SLA), sapwood-to-leaf area ratio (Huber value)]. This enabled us to explore the stringency of stomatal regulation in relation to leaf water potential variation and branch embolism resistance of the three species. The study was conducted in the upper sun crown of mature trees growing in close vicinity to each other that were accessed with a mobile skyjack. We tested the hypotheses that (1) the conifers *P. abies* and *P. menziesii* display a more isohydric regulation strategy, while *F. sylvatica* pursues an anisohydric regulation, tolerating larger Ψ_{Leaf} fluctuation, and (2) hydraulic safety margins decrease in the sequence *P. menziesii* > *P. abies* > *F. sylvatica*, since embolism resistance seems to decrease in this sequence, while the threat of encountering low water potential minima should increase. We define drought resistance in general as the ability of a plant to maintain fitness in the face of climatic and edaphic drought stress through mechanisms that help avoiding and/or tolerating tissue desiccation.

Materials and methods

Study site

The study was carried out in the Lüß Forest close to Unterlüß (Lüneburg Heath, northern Lower Saxony) in northern Germany (52°50′N, 10°19′E; elevation: 132–139 m a.s.l.). The region is characterized by a cool-temperate climate with a mean annual temperature of 9.0 °C and mean annual precipitation of 747 mm (DWD, German Weather Service, Offenbach, Germany, period 1981–2018). Soils are spodo-dystric Cambisols developed in sandy to loamy deposits of the penultimate (Saale) glaciation (Drenthe stadial) (6% clay, 15% silt, 79% sand) (Foltran et al., unpubl data). We chose stands of the three species *F. sylvatica*, *Picea abies* and *P. menziesii* in vicinity to each other (maximum distance: 2200 m) under comparable environmental conditions (Fig. S1). The physiological measurements were conducted in three mature neighboring trees per species that grew either in pure stands or mixtures with clear dominance of the respective species. The three trees each were located directly adjacent to each other and, thus, could be accessed with the skyjack within short time. All trees were of mature age (*F. sylvatica* and *P. abies*: 122 years, *P. menziesii*: 70 years), dominant individuals in the stands and in good health, with heights of 28–42 m and diameters at breast height (DBH) of 52–80 cm (Table 1). Tree height was measured in 2018 with a Vertex IV Hypsometer with T3 transponder (Haglöf, Längsele, Sweden) and DBH with a dendrometer band (UMS GmbH, München, Germany). The *F. sylvatica* stand had a mean DBH (all stems included) of 26.5 cm (range 7.2–59 cm), a basal area of 30.4 m^2 ha^{-1}, and a stem density of 320 ha^{-1}. The *P. menziesii* stand had a mean DBH of 43.6 cm (range 11.8–64.3 cm), a basal area of 50.2 m^2 ha^{-1}, and a stem density of 264 ha^{-1}. Finally, the *P. abies* stand had a mean DBH of 44.9 cm (range 12.8–66.4 cm), a basal area of ca. 30 m^2 ha^{-1}, and a stem density of 320 ha^{-1}. The stands differ mainly with respect to the number of juvenile trees, which are higher in the *F. sylvatica* and *P. menziesii*

Table 1 Structural characteristics of the nine investigated trees in 2018.

Species	Tree no.	Age (yr)	DBH (cm)	H (m)
F. sylvatica	1	122	59.8	32.4
F. sylvatica	2	122	56.0	31.1
F. sylvatica	3	122	58.0	33.8
P. abies	1	122	55.5	28.5
P. abies	2	122	52.2	28.1
P. abies	3	122	52.3	29.3
P. menziesii	1	70	57.4	37.8
P. menziesii	2	70	59.8	41.9
P. menziesii	3	70	79.5	42.3

stands. Hourly measured air temperature, air humidity, and precipitation data were obtained from a climate station set-up on an open field in close proximity to the study sites (52°49.830″N, 10°18.864″E). Vapor pressure deficit (VPD) was derived from air humidity and air temperature using the Teten's formula. Volumetric soil water content was measured with TDR- and TensioMark-sensors at 5 cm, 20 cm, 50 cm, and 100 cm depth at a station located between the *F. sylvatica* and *P. abies* stand. The nearby *P. menziesii* stand stocked on soil of similar soil texture, and soil moisture conditions were, therefore, largely comparable. Additionally, daily precipitation data were available from a gauge installed on a nearby farm (52°49′42.5″N 10°14′55.9″E).

Stomatal conductance and leaf water potential measurements

All measurements were carried out on twigs and leaves of the fully sun-exposed upper crown. In case of *F. sylvatica* and *P. abies*, this were the uppermost twigs of the crown, in case of taller *P. menziesii*, we measured side branches in the uppermost third of the crown. Canopy access was achieved through a mobile skyjack (model DL30, DENKA-Lift A/S, Denmark), which allowed reaching 30 m height. Stomatal conductance (g_S) and leaf water potential (Ψ_{Leaf}) measurements were carried out in diurnal measuring campaigns from 8 a.m. to 5 p.m. at time steps of about 1 h on various days between May and September 2018 (7–11 campaigns per species) and 2019 (4 campaigns per species). Midday leaf water potential (Ψ_{MD}) and midday stomatal conductance (g_{MD}) measurements were taken between 12 a.m. and 4 p.m. on sunny or partly cloudy days, and daily minima were identified from those values separately for each year. The three lowest Ψ_{Leaf} values recorded in a summer were averaged and termed Ψ_{min}. Stomatal conductance was measured with a Li-Cor 6400 gas exchange system (Li-Cor Inc., Lincoln, NE, USA) at ambient light, air humidity, and temperature conditions. The skyjack was placed in the center of the three studied trees of the same species, and each five leaves (or needle-bearing shoots) per tree on the same twig were measured every hour, rotating between the three trees each. We then averaged over the 15 measurements per hour and tree species. As the skyjack could not be moved so rapidly to accommodate all 9 trees of the three species on the same day, the three species were measured on different days, usually on the next days. Since all measuring days were sunny or partly overcast days, the atmospheric conditions on consecutive days were sufficiently comparable. Due to the hot and dry weather in the summers of 2018 and 2019, the majority of leaf conductance measurements were conducted under photon flux densities close to or above light saturation of photosynthesis of the species (c. 450–700 µmol m^{-2} s^{-1}; Leuschner and Ellenberg 2017).

While *F. sylvatica* leaves were measured in the conventional leaf chamber (which was completely filled by the leaves), we used the conifer chamber for measurements on *P. menziesii* and *P. abies* short shoots. To relate photosynthesis to area, the cumulative needle surface area of all needles inside the chamber was determined with the software WinSeedle 2013 (Régent Instruments, Quebec City, QC, Canada). This was determined for each three shoots of a tree, and the area averaged. All leaves were marked at the beginning of the season to ensure that measurements always took place on the same leaves/shoots throughout the summer. In case of leaf damage or loss, it was replaced by another leaf on the same branch. We measured in both seasons (2018 and 2019) the same branches.

Ψ_{Leaf} was measured with a Scholander pressure chamber (1505D-EXP, PMS Instruments Company, Albany, OR, USA) on short shoots of *F. sylvatica* (typically bearing four leaves), *P. abies,* and *P. menziesii* (youngest shoots of ca. 10 cm length). We measured three leaves/shoots (one per tree) for Ψ_{Leaf} per hour and averaged the data. The shoots used for Ψ_{Leaf} measurement were taken from a branch in direct neighborhood to the one serving for stomatal conductance measurements. To characterize the three species along the isohydry–anisohydry continuum of water potential variation (Klein 2014), we chose the seasonal variability of Ψ_{MD} as a criterion, with more isohydric species showing less variability (Martinez-Vilalta and Garcia-Forner 2017).

Measurement of xylem hydraulic conductivity and vulnerability curves

During the second half of August in 2018 and 2019, each 6–8 sun-canopy branches per species of about 50 cm length and 10 mm in diameter were collected for hydraulic conductivity measurements and analysis of vulnerability curves. The branches were cut in the air and immediately wrapped in moist towels, which had been soaked in distilled

water containing a sodium–silver-chloride complex (16 µg L^{-1} Ag and 8 mg L^{-1} NaCl; Micropur katadyn, Wallisellen, Switzerland) to restrict microbial activity. The samples were stored at 4 °C in the dark and used for hydraulic conductivity measurement and vulnerability curve establishment within 4 weeks. The twig segment used for conductivity measurement was marked in the field and all leaves distal to the segment were collected and stored in plastic bags at 4 °C. Additional branch samples (two per tree, i.e., six per species) were collected at the end of August 2018 in the sun canopies for establishing pressure–volume curves. The twigs were cut in the field and immediately transferred to polyethylene tubes containing demineralized water and covered with a plastic bag to prevent water loss, were re-cut under water in the laboratory and stored overnight in a cool and dark room (Koide et al. 2000; Prometheuswiki 2018).

Hydraulic conductivity (K_h, kg m MPa^{-1} s^{-1}) was determined on 3–4 branches per tree by connecting the segment to the Xyl'em apparatus (Bronkhorst, Montigny-les-Cormeilles, France) and flushing demineralized, degassed and filtered (0.2 µm) water containing 10 mM KCl and 1 mM $CaCl_2$ through the segment. We used different procedures for broadleaved *F. sylvatica* and the conifers. In case of *F. sylvatica*, branches were shortened under water to about 30 cm length, lateral branches were cut-off and the scars quickly sealed with instant glue (Loctite 431, Henkel, Düsseldorf, Germany) to prevent water leakage during measurement. The exact length of the segments and their diameters were measured twice at the basipetal and distal ends and four times along the segment. Subsequently, 1 cm of the bark at the basipetal end was removed and the twigs connected to the Xyl'em apparatus. After obtaining the actual hydraulic conductivity (K_h^{act}) under a small pressure difference of 6 kPa, samples were flushed at high pressure (120 kPa) for 10 min to remove potential emboli. Measurements at low pressure and flushing events were repeated until maximum hydraulic conductivity (K_{hmax}) was reached. In case of the conifers, branches were shortened under water to a segment length of 5 cm that lacked lateral branches, and the bark was completely removed. Length and diameters were measured in the same way as for *F. sylvatica*. To avoid conduit sealing by resin released during flushing, samples were afterward stored under vacuum for at least 12 h, while kept in the flushing solution. Subsequently, K_{hmax} was measured in the conifer samples at 6 kPa pressure. Hydraulic conductivity and flow rate were computed with the software XylWin 3.0 (Bronkhorst, Montigny-les-Cormeilles, France), which considers segment length. Specific hydraulic conductivity (K_S, kg m^{-1} MPa^{-1} s^{-1}) was computed by dividing K_{hmax} by the maximal basipetal sapwood cross-sectional area (A_{cross}^{max}) without pith and bark (Hajek et al. 2014; Schuldt et al. 2016). To obtain A_{cross}^{max} without bark for the *F. sylvatica* twigs with bark, the following equation established by Schuldt et al. (2016) was used: $A_{cross}^{max} = -3.715 + (0.7698 * A_{cross}^{max}\ (bark))$, with A_{cross}^{max} (bark) being the recorded A_{cross}^{max} including bark. Leaf-specific conductivity (K_L, kg m^{-1} MPa^{-1} s^{-1}) was calculated by dividing K_{hmax} by the associated total leaf area of the branch segment.

For establishing vulnerability curves, the Cavitron technique was applied (Cochard et al. 2005), using a custom-made Cavitron rotor chamber (Delzon et al. 2010) attached to a commercially available centrifuge (Sorvall RC-5C; Thermo Fisher Scientific, Waltham, MA, USA). In *F. sylvatica*, an average maximum vessel length of 19.3 ± 2.6 cm has been reported (Lübbe et al. 2022), which makes this species suited for flow-centrifuge measurements with a 30 cm rotor. Three–four branches per species were cut under water to a length of 27.5 cm, and the bark removed at both ends for about 3 cm in case of *F. sylvatica*, or completely in case of the conifers, before cutting to avoid possible extrusion of resin. Conductivity measurements started with a negative pressure of − 0.83 MPa, and pressure was raised stepwise by 0.2–0.3 MPa until a percentage loss of conductance (PLC) of at least 90% was reached. PLC values were recorded with the software CaviSoft (Version 2.1, University of Bordeaux, France) and plotted against xylem pressure to generate vulnerability curves. To derive the xylem pressure causing 50% loss of conductance (P_{50}), a sigmoidal function was fitted to the data points according to the equation given by Pammenter and Vander Willigen (1998), with $PLC = 100/(1 + \exp(s/25 * (P_i - P_{50})))$, in which s (% MPa^{-1}) is the negative slope of the curve at the inflexion point and P_i the applied xylem pressure. The xylem pressures causing 12% (P_{12}; embolism onset) and 88% (P_{88}) loss of conductance were derived following Domec und Gartner (2001) with $P_{12} = 2/(s/25) + P_{50}$ and $P_{88} = -2/(s/25) + P_{50}$.

Establishment of pressure–volume curves

Pressure–volume curves (PVC), i.e., the plot of water potential ($-1/\Psi$ in MPa) vs. 100 − total relative water content (RWC, %), were established in twigs sampled at the end of August 2018 with the over-pressurization technique (Tyree and Jarvis 1982; Koide et al. 2000) using several pressure chambers (1505D-EXP and M1000, PMS Instruments Company, OR, USA). Measurements took place on the day after sampling on two twigs per tree (six per species) that had been hydrated to near-maximum turgor overnight and that were measured in parallel, following the protocol given by Leuschner et al. (2019). Briefly, samples were once more re-cut before measurement, dried with tissue paper, weighed to 1 µg to determine initial fresh weight and immediately placed in the pressure chamber to measure the initial water

potential. The pressure in the chamber was then increased to 0.4 MPa and kept at this level for 10 min. while the expressed sap was collected in a small vial filled with cotton wool. Subsequently, the pressure was released for 10 min to allow symplast and apoplast to equilibrate. This procedure was repeated in pressure steps of 0.3 MPa until 2.5 MPa were reached. To achieve a higher resolution in the linear part of the pressure–volume curve, the steps were reduced to 0.2 MPa between 2.5 and 3.3 MPa (final value). The vials were weighed to an accuracy of 100 µg before and after collecting the sap for calculating the amount of expressed sap. Finally, the leaves and shoots were dried at 70 °C for 48 h to determine dry weight. The following parameters were derived from the curves: osmotic potential at full turgor (π_0) and at turgor loss point (π_{tlp}), relative water content (symplastic water) at full hydration (RWC_0), relative water content at turgor loss point (RWC_{tlp}), and the bulk modulus of tissue elasticity (ε_0) with ε_0 being calculated with the standard major axes method (Sokal and Rohlf 1995).

Leaf morphological measurements

All leaves and needles on the measured twigs were scanned (V11 Epson Perfection, Epson, Nagano, Japan) and analyzed with the software WinFolia 2005 (Régent Instruments, Quebec City, QC, Canada) in case of leaves and WinSeedle 2013 (Régent Instruments, Quebec City, QC, Canada) in case of needles to obtain mean leaf/needle area and total leaf area on the twig (A_{mean} and A_{total}, cm^2). To overcome the problem of comparing leaf and needle surface areas, we used projected surface area (silhouette area) for both types of foliage in subsequent calculations (e.g., for stomatal conductance), as has been done in earlier studies (e.g., Wallin et al. 1990; Stinziano et al. 2015). The option to calculate total surface area (upper and lower side) of the needles from the measured projected area by means of empirically determined factors (Keller and Wehrmann 1963; Perterer and Körner 1990; Goisser et al. 2016) was abandoned, as it would have inflated the foliage surface area of the conifers compared to *F. sylvatica*, and due to considerable variation in conversion factors, which vary between 2.38 (Schulze et al. 1977) and 3.2–3.3 (Perterer and Körner 1990; Goisser et al. 2016), probably due to the influence of local environmental conditions.

We further calculated Huber value (HV, 10^4 m^2 m^{-2}), i.e., the sapwood-to-leaf area ratio, by dividing sapwood cross-sectional area (see above) by the total leaf area distal to the cut. Leaves were oven-dried at 70 °C for 48–72 h and subsequently weighed to calculate specific leaf area (leaf surface to dry mass ration, SLA, in cm^2 g^{-1}).

Statistical analysis

All statistical analyses were carried out with the software package R (R Core Team 2013, version 4.0.5), except for the determination of $P_{12/50/88}$-values, which were calculated with SAS 9.13 software (SAS Institute Inc., Cary, North Carolina, USA). Subsamples from a tree were averaged and the data subsequently tested for normal distribution with a Shapiro–Wilk normality test. The Wilcoxon signed-rank test was used to test for significant differences in the studied traits, comparing years and species based on means at the tree level (see Table 2). Linear models were fitted to the data after selection of the best-fitting model using the Akaike Information Criterion (AIC) and the model results depicted in the graphs. A significance level of $p < 0.05$ was used throughout the paper.

Results

Weather and soil moisture conditions in 2018 and 2019

While both summers 2018 and 2019 were exceptionally dry and hot, the two years differed in the timing of dry and moist periods. The summer 2018 was characterized by a very long period without larger rainfall events (no single event with > 13 mm d^{-1} between mid of April and September, rainfall total May–September: 94 mm, annual precipitation total: 435 mm). Soil water content varied in the whole profile to 1 m depth around 2 vol.% until October (maximum: 3%), and maximum air temperature reached 36.3 °C, minimum relative air humidity 22% and maximum VPD 4.3 kPa (Fig. S2 in the Supplement). Precipitation in summer was somewhat higher in 2019 (284 mm from May to September), but soil moisture reserves had not been recharged during the 2018/2019 winter, and soil water content consequently reached only 13 vol.% in mid-March 2019, to drop to 3 vol.% in early July. As in summer 2018, relative air humidity dropped to 21% in summer 2019, maximum air temperatures reached 37.3 °C and maximum VPD 4.7 kPa.

VPD dependence of stomatal conductance

Stomatal conductance (g_S) was relatively low in 2018 in all three species with most values ranging between 15 and 100 mmol m^{-2} s^{-1} only (Fig. 1). Higher g_S values (up to 220 mmol m^{-2} s^{-1} in *F. sylvatica* and to 170 mmol m^{-2} s^{-1} in the conifers) were reached in all species in 2019, with the increase being most pronounced in *F. sylvatica*. g_S was in both summers higher in *F. sylvatica* (68:9 ± 43.6 mmol m^{-2} s^{-1}) than in the two conifers (*P. abies*: 32.3 ± 40.2 mmol m^{-2} s^{-1}; *P. menziesii*: 24.0

Table 2 Physiological and leaf morphological traits of the three species in the summers 2018 and 2019 (species-level means with SE in brackets)

Trait	Units	*Fagus sylvatica*		*Picea abies*		*Pseudotsuga menziesii*	
		2018	2019	2018	2019	2018	2019
K_s	kg m^{-1} MPa^{-1} s^{-1}	**1.56 ± 0.13** a	**0.84 ± 0.07** A	**0.66 ± 0.10** b	**0.48 ± 0.13** B	**0.48 ± 0.02** c	**0.34 ± 0.02** C
K_L	10^{-4} kg m^{-1} MPa^{-1} s^{-1}	2.76 ± 0.87 a	3.05 ± 1.02 A	**0.34 ± 0.07** b	**1.30 ± 0.39** B	**0.28 ± 0.08** b	**0.48 ± 0.06** C
A	cm^2	**14.49 ± 2.70** a	**7.14 ± 1.63** A	0.15 ± 0.02 b	0.14 ± 0.01 B	0.27 ± 0.06 c	0.25 ± 0.05 C
SLA	cm^2 g^{-1}	**150.39 ± 10.76** a	**128.35 ± 6.48** A	**50.01 ± 9.76** b	**39.81 ± 2.25** B	88.15 ± 7.63 c	83.10 ± 7.06 C
HV	10^{-4} m^2 m^{-2}	**1.81 ± 0.46** a	**3.62 ± 1.07** A	**1.18 ± 0.24** b	**2.70 ± 0.56** A	1.24 ± 0.38 b	1.50 ± 0.24 B
P_{50}	MPa	**− 3.75 ± 0.21** a	**− 3.28 ± 0.16** A	− 3.61 ± 0.11 ab	− 3.48 ± 0.17 A	− 3.40 ± 0.37 b	− 3.36 ± 0.41 A
P_{12}	MPa	**− 3.22 ± 0.27** a	**− 2.56 ± 0.22** A	− 2.86 ± 0.04 a	− 2.56 ± 0.13 A	− 2.85 ± 0.28 a	− 2.57 ± 0.27 A
P_{88}	MPa	**− 4.29 ± 0.20** a	**− 4.01 ± 0.20** A	− 4.37 ± 0.24 a	− 4.40 ± 0.22 B	− 3.95 ± 0.49 a	− 4.14 ± 0.55 AB
Slope		101.21 ± 28.54 a	76.9 ± 13.99 A	74.67 ± 8.90 a	56.45 ± 7.62 B	104.70 ± 18.5 a	69.29 ± 11.88 AB
Ψ_{Min}	MPa	− 2.77 ± 0.31 a	− 2.71 ± 0.00 A	**− 2.19 ± 0.14** b	**− 2.34 ± 0.00** B	− 2.71 ± 0.10 a	− 2.54 ± 0.00 C
HSM $\Psi_{min} - P_{50}$	MPa	**0.99 ± 0.18** a	**0.58 ± 0.17** A	1.42 ± 0.16 b	1.13 ± 0.01 B	0.69 ± 0.39 a	0.85 ± 0.26 AB
HSM $\Psi_{min} - P_{12}$	MPa	**0.46 ± 0.06** a	**− 0.15 ± 0.34** A	**0.67 ± 0.18** a	**0.22 ± 0.11** A	0.14 ± 0.32 a	0.03 ± 0.28 A
HSM $P_{12} - P_{50}$	MPa	0.53 ± 0.12 a	0.73 ± 0.16 A	0.75 ± 0.13 a	0.92 ± 0.12 B	0.55 ± 0.13 a	0.78 ± 0.13 A
HSM $\Psi_{min} - P_{88}$	MPa	1.52 ± 0.29 a	1.30 ± 0.05 A	2.18 ± 0.22 b	2.05 ± 0.06 B	1.24 ± 0.49 a	1.60 ± 0.25 A

K_S specific conductivity, K_L leaf-specific conductivity. *A* leaf area, *HV* Huber value. $P_{12,\ 50,\ 88}$ xylem pressure at 12, 50 and 88% loss of conductivity, *Slope* slope of the vulnerability curve at the inflexion point, Ψ_{min} – lowest Ψ_{Leaf} value recorded in the summer (in contrast to Fig. 3, this table gives averages over the three individuals each), *HSM* safety margin calculated as xylem potential at 50, 12 or 88% percent loss of conductivity ($P_{50,12,88}$) minus minimal midday leaf water potential (Ψ_{MD}). For HSM, four alternative calculation approaches are shown with Ψ_{MD} being minimal midday leaf water potential.

Values in bold indicate significant differences between years ($p < 0.05$)

± 21.7 mmol m^{-2} s^{-1}); *P. abies* tended to have a higher stomatal conductance than *P. menziesii.* The latter species maintained especially low stomatal conductance levels in mid and late summer 2018 (16.8 ± 10.2 mmol m^{-2} s^{-1} from mid-July–September), with only minor g_S reduction upon a VPD increase. The dependence of g_S on VPD was significant in all three species in 2018, but this relation diminished (or was weak) in 2019 in *F. sylvatica* and *P. abies*. The strongest g_S decrease with VPD was recorded among the species in *F. sylvatica* in 2018 ($p < 0.001$, $R^2 = 0.45$) and in *P. menziesii* in 2019 ($p = 0.008$ and $R^2 = 0.22$), covering a VPD range of c. 0.4–2.3 kPa.

Relationships between g_S and Ψ_{Leaf}

The extent of seasonal variation in midday stomatal conductance (g_{MD}) and midday leaf water potential (Ψ_{MD}) differed markedly between the species and also between the summers. In *F. sylvatica* and *P. menziesii*, the $g_{MD} - \Psi_{MD}$ relationship was positive and highly significant, while only a non-significant tendency appeared in *P. abies* (Fig. 2). Moreover, the g_{MD} drop with a Ψ_{MD} decline was steeper in *P. menziesii* than in *P. abies* and *F. sylvatica*. *F. sylvatica* revealed in 2018 a characteristic anisohydric behavior with a marked Ψ_{MD} decline from about − 1.7 to − 2.7 MPa (Δ1 MPa) between June and September, even though midday stomatal conductance was reduced from about 70 to 20 mmol m^{-2} s^{-1}. In contrast, *P. abies* exhibited in 2018 a typical isohydric leaf water status regulation pattern with maintenance of very low g_{MD} values of 12.3 ± 11.1 mmol m^{-2} s^{-1} throughout summer, which resulted in an only minor Ψ_{MD} drop between June and September (by ca. 0.3 MPa; Fig. 3). *P. menziesii* also reached only very low g_{MD} values of 12.5 ± 7.1 mmol m^{-2} s^{-1} between July and September, and showed minimal change in Ψ_{MD} (Δ 0.1 MPa), but it is likely that water potential has dropped from higher levels already in May or June. Patterns were different in summer 2019, when all three species showed a linear decline in leaf water potential from May to October. Daily Ψ_{Leaf} and g_s minima started at higher levels in summer 2019 than in 2018, and the seasonal Ψ_{MD} drop was larger in *P. abies* in 2019 than in 2018 (Δ1.0 MPa vs. 0.3 MPa). g_{MD} declined from early to late summer only in *P. abies*, but reached a late-summer peak in *F. sylvatica* and *P. menziesii*, surpassing 100 mmol m^{-2} s^{-1} (Fig. 3).

Diurnal Ψ_{Leaf} drops were in *F. sylvatica* usually associated with reductions in stomatal conductance (positive $\Psi_{Leaf} - g_S$ relationship), but negative relations were also recorded in the summers 2018 and 2019, demonstrating the complexity of this interaction (Fig. S3 in the Supplement). Both negative and positive $\Psi_{Leaf} - g_S$ relationships were also observed in *P. abies* and *P. menziesii* on the diurnal scale, but the

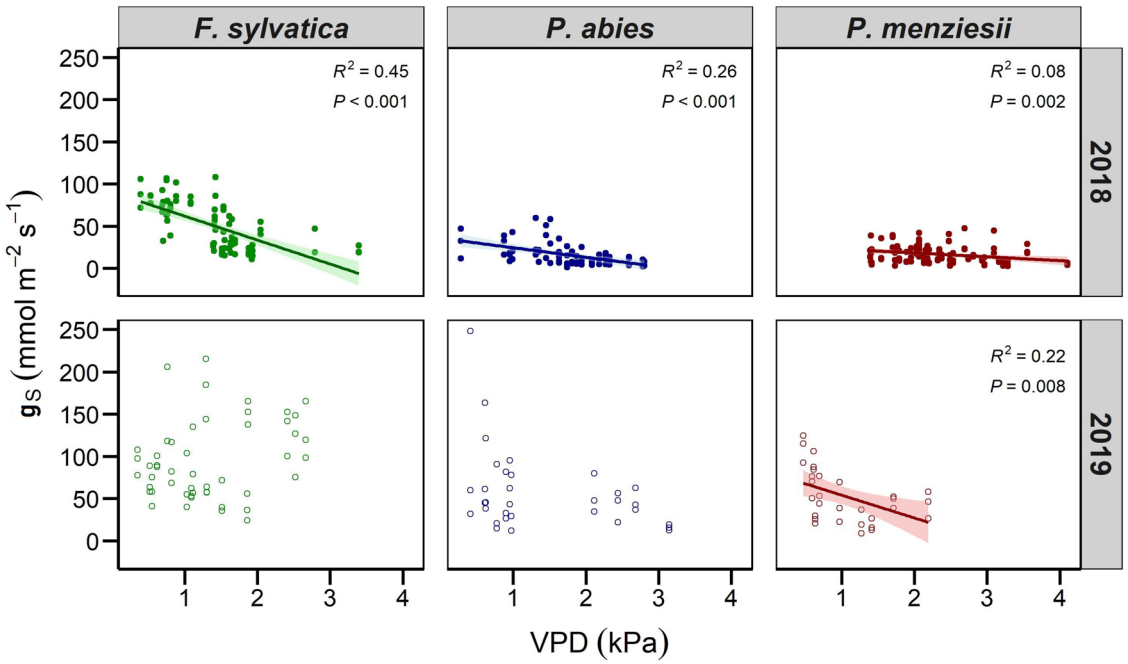

Fig. 1 Dependence of leaf stomatal conductance (g_S) on vapor pressure deficit of the air (VPD) in summer 2018 and 2019 for the three species (all measurements taken between 10 a.m. and 4 p.m. on various sunny or overcast days between June and September). Each point represents the mean of five replicate leaves/shoots measured per tree. R^2 and p values are given for each curve per species per year. Only significant relationships are displayed with regression lines

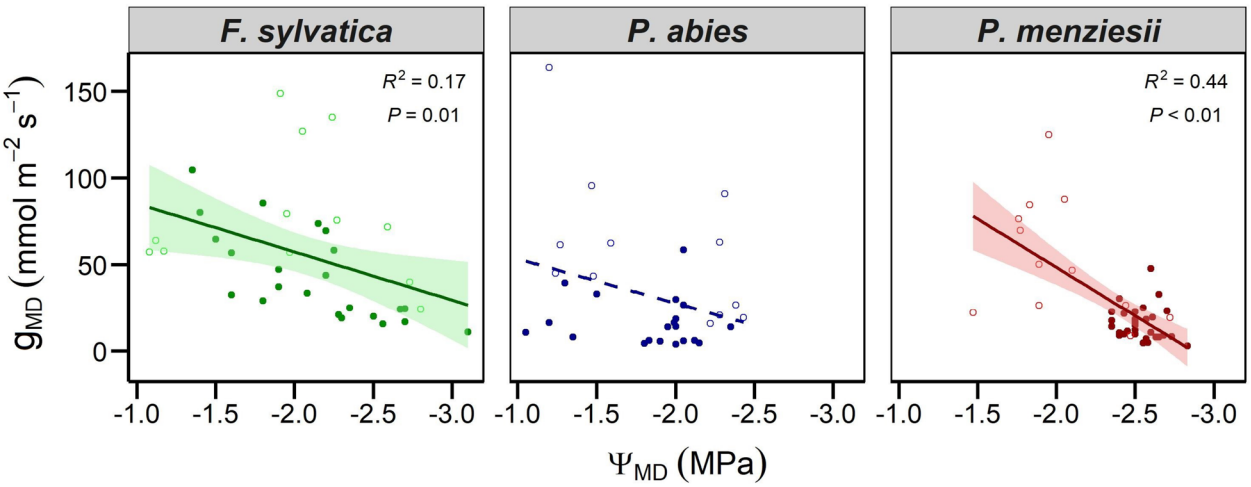

Fig. 2 Relationship between midday leaf conductance (g_{MD}) and midday leaf water potential (Ψ_{MD}) in 2018 (filled symbols) and 2019 (open symbols) in the three species. Each point gives a day's leaf conductance at the time of daily leaf water potential minimum (Ψ_{MD}) (g_{MD} values are means of each five replicate leaves measured per tree, while Ψ_{MD} values base on one measurement only). *F. sylvatica*: $y = 113 - 27.9x$, *P. menziesii*: $y = 160 - 55.9x$. Regression lines base on the pooled data of the two summers. Significant R^2 and p values are given for each line per species

g_S range was generally smaller than in *F. sylvatica*. Positive relationships prevailed in the conifers especially in late summer (August and September). All three species showed a remarkable increase in maximum g_S in 2019 compared to 2018 (*F. sylvatica*: from ~ 120 to ~ 215 mmol m^{-2} s^{-1}; *P. abies*: from ca. 50 to ca. 160 mmol m^{-2} s^{-1}; *P. menziesii*: from 47 to 125 mmol m^{-2} s^{-1}, Fig. S3).

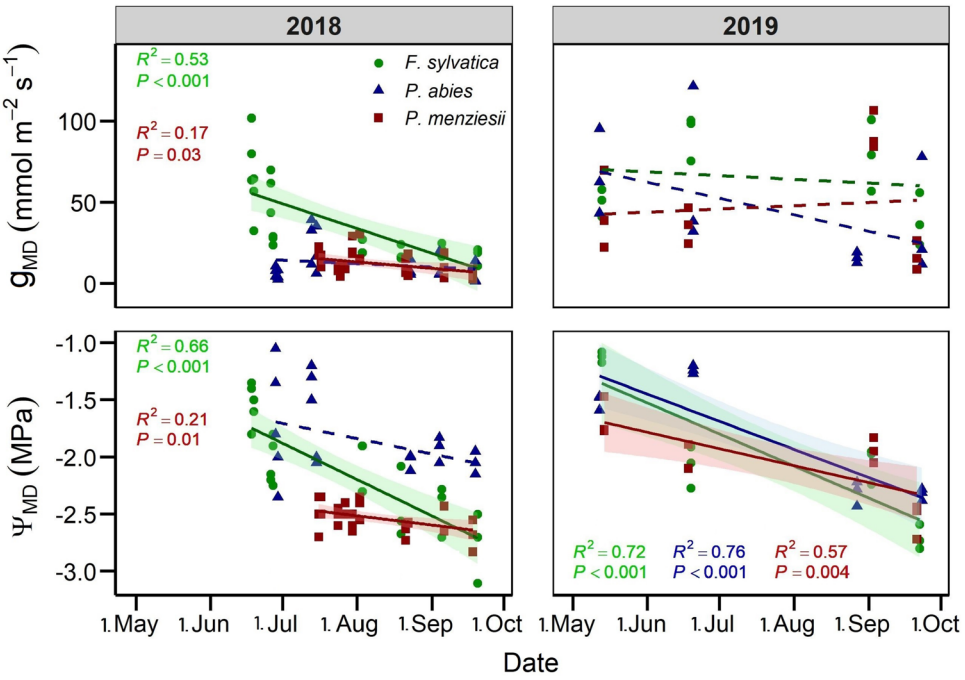

Fig. 3 Seasonal variation in daily stomatal conductance minimum (g_{MD}) and leaf water potential minimum (Ψ_{MD}), according to measurements between 12 p.m. and 4 p.m. on several days from May until September 2018 and 2019. Each point shows one value per day per tree, whereas values of g_S are means of 5 replicate leaves per tree. R^2 and p values are given for each curve per species per year. Dots and lines in green: *F. sylvatica,* in blue: *P. abies,* in red: *P. menziesii*

Pressure–volume curve parameters

Sun-crown foliage sampled during peak drought in late August 2018 showed for the three species remarkably similar leaf tissue osmotic potentials at full turgor (π_0; range of species means: −2.05 to − 2.12 MPa) and at turgor loss (π_{tlp} − 2.44 to − 2.51 MPa), relative water content at turgor loss point (RWC_{tlp}; 0.88–0.90) and of the bulk tissue elastic modulus at maximum turgor (ε_{max}; 15.04–21.43 MPa) (Fig. 4). Significant differences between species were only found for ε_{max}, and a weak tendency toward a more negative π_{tlp} in *P. abies*.

Xylem embolism resistance and stomatal closure

Although the P_{50}-values were fairly similar among the three species, the vulnerability curves revealed a tendency toward earlier embolism onset (P_{12}) in the conifers than in *F. sylvatica* in the 2018 samples (Fig. 5). However, after a shift toward less negative P_{12}-values (and in *F. sylvatica* also: P_{50}-values) in 2019, these species differences diminished. While the conifers showed only minor inter-annual change in embolism resistance, it appears that *F. sylvatica* was less resistant in 2019 than in 2018 (Table 2).

In summer 2018, stomatal closure (assumed for $g_{s95\%}$, i.e., 5% of maximum measured g_s) occurred at leaf water potentials close to the P_{12}-value in *F. sylvatica* (~ − 3.15 MPa) and *P. menziesii* (~ − 2.8 MPa), while *P. abies* closed its stomata well in advance of the onset of embolism (~ − 2.15 MPa). The P_{12}-value shift to higher xylem water potentials and, thus, greater embolism vulnerability in *F. sylvatica* in 2019 resulted in a drop of the Ψ_{Leaf} value at stomatal closure below the species' P_{12} threshold, even though *F. sylvatica* closed its stomata at higher leaf water potentials in 2019 (~ − 2.85 MPa) than in 2018 (~ − 3.20 MPa). In 2019, *P. abies* closed stomata later (~ − 2.5 MPa) than in 2018 (~ − 2.15 MPa), which, therefore, corresponded with the shifted onset of embolism. *P. menziesii* apparently closed its stomata also more sensitively in 2019 (at ~ − 2.65 MPa) than in 2018, maintaining the association of stomatal closure with the P_{12}-value (Fig. 5).

In 2018, hydraulic safety margins (HSM) were largest in *P. abies* (1.42 MPa), intermediate in *F. sylvatica* (0.99 MPa) and smallest in *P. menziesii* (0.69 MPa) (Fig. 6). However, HSM changed from 2018 to 2019 due to shifts in P_{50} and observed Ψ_{min}-values. While *P. menziesii* kept its HSM relatively constant with only a slight increase to 0.85 MPa, *P. abies* and *F. sylvatica* reduced their HSM to 1.13 MPa and 0.58 MPa, respectively, leaving *F. sylvatica* in 2019 with the smallest HSM of the three species (Table 2, Fig. 6).

Inter-annual variation in physiological and leaf morphological traits

The comparison of species-level leaf and xylem traits between the two years revealed high inter-annual variation in *F. sylvatica*, medium variation in *P. abies,* and low variation in *P. menziesii* (Table 2). All three species had a significantly lower xylem-specific hydraulic conductivity (K_S) in 2019

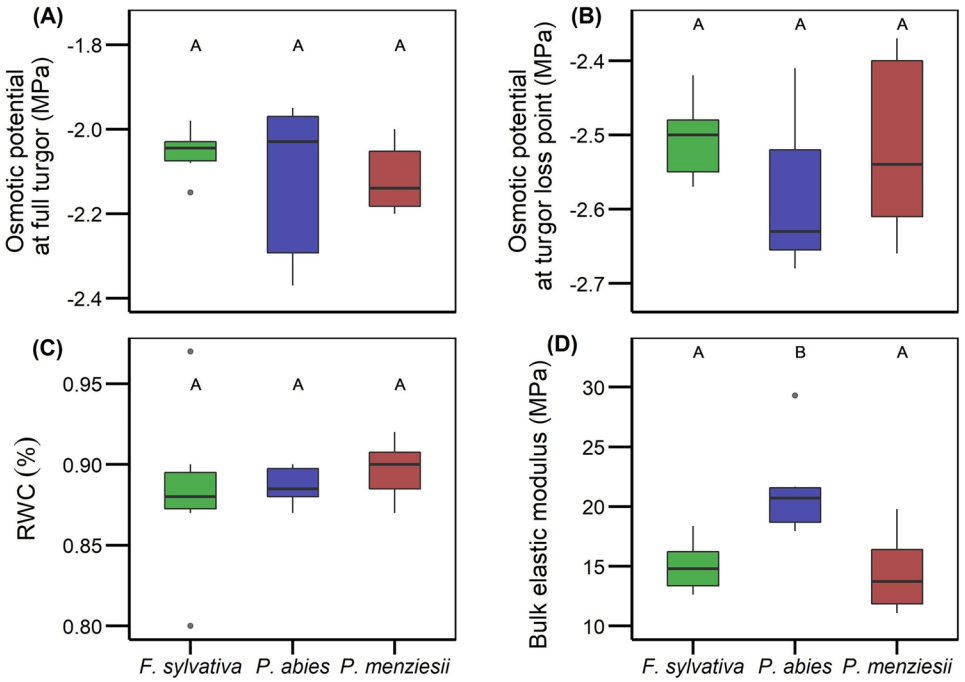

Fig. 4 Osmotic potential at **a** full turgor (π_0) and **b** at turgor loss point (π_{tlp}), **c** relative water content at turgor loss point (RWC), and **d** bulk tissue modulus of elasticity at full turgor (ε_{max}) ($n = 6$). Different capital letters indicate significant differences between species ($p < 0.05$)

than in 2018, while leaf area-specific conductivity (K_L) increased toward 2019 in the conifers (significant) and in *F. sylvatica* (non-significant). While *P. menziesii* showed no inter-annual variation in all other investigated traits, *P. abies* and *F. sylvatica* reduced specific leaf area (SLA) and leaf size (*A*) (only *F. sylvatica*) but increased Huber value (HV) from 2018 to 2019. P_{12}-, P_{50}- and P_{88}-values were significantly higher (less negative) in 2019 in *F. sylvatica* but not in the conifers. Hydraulic safety margins (HSM), as calculated with $\Psi_{min,}$ were significantly reduced in 2019 in *F. sylvatica* and *P. abies* but not in *P. menziesii*.

Discussion

Our results on seasonal Ψ_{MD} variation during the summers 2018 and 2019 support the conclusion of earlier studies (Backes and Leuschner 2000; Köcher et al. 2009; Leuschner et al. 2021; Walthert et al. 2021) that *F. sylvatica* pursues a strictly anisohydric strategy, supporting our first hypothesis. In our study, sun-leaf Ψ_{MD} varied by > 2 MPa (from c. − 0.7 to − 3.1 MPa) between June and September 2018, and by 2 MPa (− 0.8 to − 2.8 MPa) from May to September 2019. An even larger seasonal leaf water potential amplitude (> 2.5 MPa) has been recorded in Swiss *F. sylvatica* trees during the extreme 2018 drought (Walthert et al. 2021; Kahmen et al. 2022), when absolute Ψ_{MD} minima of − 3.3 MPa were reached in sun-exposed branches. From a literature review, it appears that Ψ_{MD} of adult *F. sylvatica* trees drops below − 2.7 MPa only during exceptional droughts as in 2018 (Leuschner 2020), while seasonal variation in normal years is usually smaller.

While *P. abies* revealed in 2018 a characteristic isohydric regulation with only minor seasonal drops in Ψ_{MD} from July to October ($\Delta \sim 0.3$ MPa), it seems that the species' isohydric strategy failed with the extension of the drought into 2019, and spruce apparently shifted in summer 2019 toward a more anisohydric behavior with a pronounced Ψ_{MD} decrease ($\Delta \sim 1.0$ MPa) from May to September, similar to the potential drop observed in *F. sylvatica*. The isohydric behavior of *P. abies* is well documented (Lyr et al. 1992; Hartmann et al. 2013; Leo et al. 2014; Oberhuber et al. 2015) and meets the assumption that conifers often have a more stringent stomatal regulation with earlier stomatal closure upon water deficits than angiosperm trees (Zweifel et al. 2007; McDowell et al. 2008; Carnicer et al. 2013). However, Ψ_{MD} has been found to vary largely between sites and years across European *P. abies* populations, suggesting that the stringency of leaf water potential regulation may depend partly on local environmental conditions. We measured in *P. abies* Ψ_{MD} minima of − 2.35 and − 2.40 MPa in 2018 and 2019, which compares well with the minimum of − 2.50 MPa recorded by Lu et al. (1995) in the Vosges Mountains, France. In contrast, Schuldt et al. (2020) reported Ψ_{Leaf} minima up to − 4.20 MPa in this species in the very dry summer of 2018 in certain Central European stands, which later succumbed to death.

For *P. menziesii*, evidence of both isohydric (Bansal et al. 2015; Voelker et al. 2018) and more anisohydric

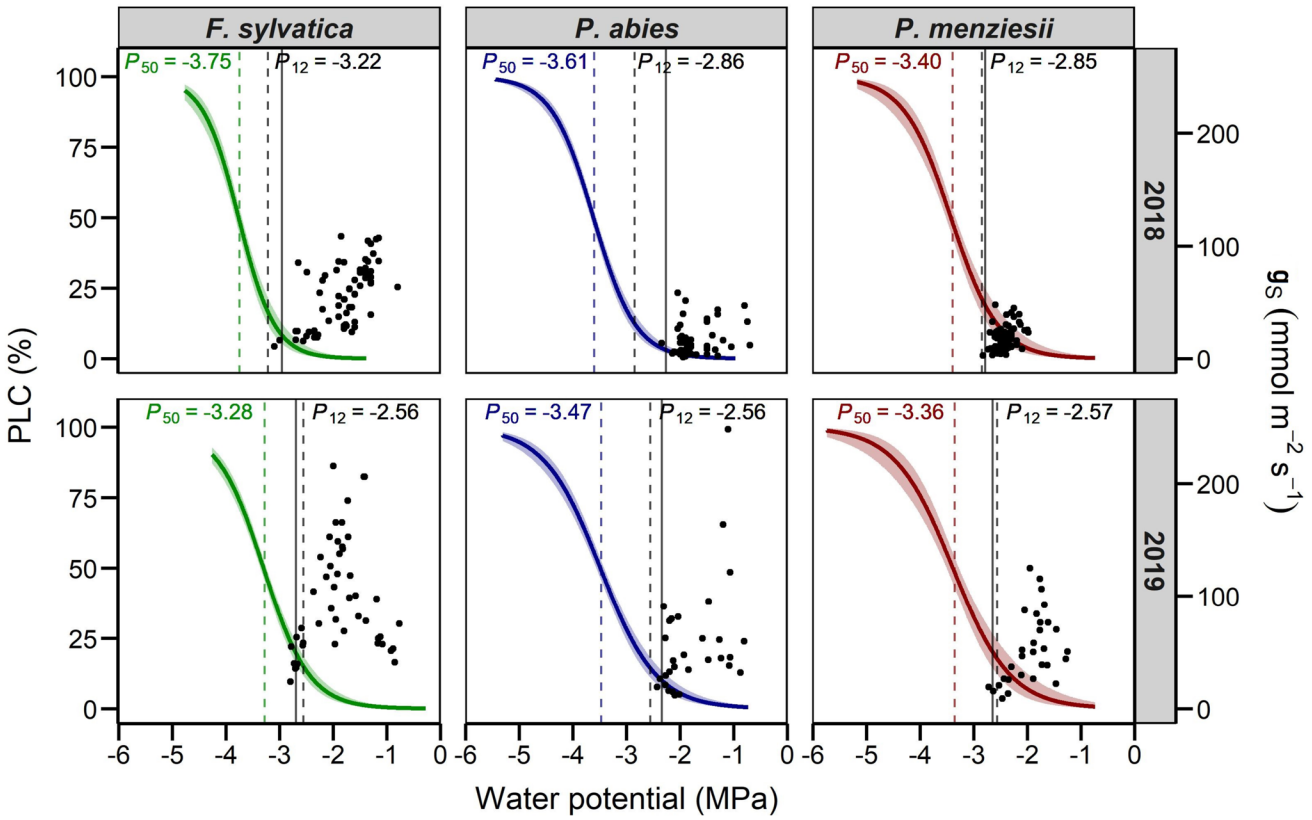

Fig. 5 Relationships between stomatal conductance (g_S) and leaf water potential (Ψ_{Leaf}) (black dots, right *y* axis) (measured between 10 a.m. and 4 p.m. from June to September 2018 and 2019), and between percentage loss of hydraulic conductivity in branch xylem (PLC) and leaf water potential (Ψ_{Leaf}) (vulnerability curves at the species level; colored curves; left *y* axis) for the three species in 2018 and 2019. Each point represents the mean of 5 replicate leaves per tree. Shaded areas around VCs indicate 95% confidence interval of means. Dashed lines indicate P_{12}- and P_{50}-values, i.e., xylem pressures with 12% or 50% loss of conductivity, and the solid line shows the point of stomatal closure. Vulnerability curves and P_{12}- and P_{50}-values are means of the three measured trees per species and the each 3–4 replicate samples per tree. We assumed stomatal closure to have occurred at g_S values equaling 5% of maximum g_s recorded in the two years ($g_{s95\%}$). Stomatal closure occurring close to P_{12} hints at possible interactions between stomatal closure and the onset of embolism

behavior (Phillips et al. 2002; Warren et al. 2003; Jansen 2017) has been reported. Our results show a Ψ_{MD} decrease by ~ 0.6 MPa in summer 2019 and hint at a larger Ψ_{MD} drop also in early summer 2018 (for which we have no data), suggesting a more anisohydric regulation, even though less pronounced than in *F. sylvatica*. The few available water potential measurements on mature *P. menziesii* trees show only moderate seasonal reductions in Ψ_{MD} to around − 2.2 to − 2.6 MPa (Brix and Mitchell 1986; Andrews et al. 2012) or ~ − 2.1 MPa (Running 1976) in North American stands differing in annual precipitation, suggesting an intermediate position on the iso/anisohydric axis.

It appears that tree species can exhibit considerable intraspecific variation in the degree of isohydry and, therefore, typically cannot be characterized as strictly anisohydric or isohydric (Cocozza et al. 2016). It seems likely that most tree species with a somewhat broader hydrological and climatic niche are exhibiting a certain degree of plasticity in their stomatal regulation strategy, allowing for shifts along the isohydry–anisohydry continuum in dependence on water availability, temperature, development stage and other cues. This suggests adopting a more dynamic picture of the stomatal regulation strategy of trees than is conventionally done.

All three species showed a relatively small stomatal conductance in the two summers relative to literature data, reflecting the exceptional drought and heat in 2018 and 2019. g_S values of *F. sylvatica* sun-crown leaves remained < 150 mmol m^{-2} s^{-1} in 2018 and < 200 mmol m^{-2} s^{-1} in 2019, which is well below the range of reported daily maximum g_S values of up to 300 mmol m^{-2} s^{-1} for this species (Leuschner 2020; Leuschner et al. 2021). Similarly, *P. abies* and *P. menziesii* reached only relatively low maximum g_S values in 2018 and 2019 at our site (in most cases < 180 and < 130 mmol m^{-2} s^{-1}, respectively). In the exceptionally

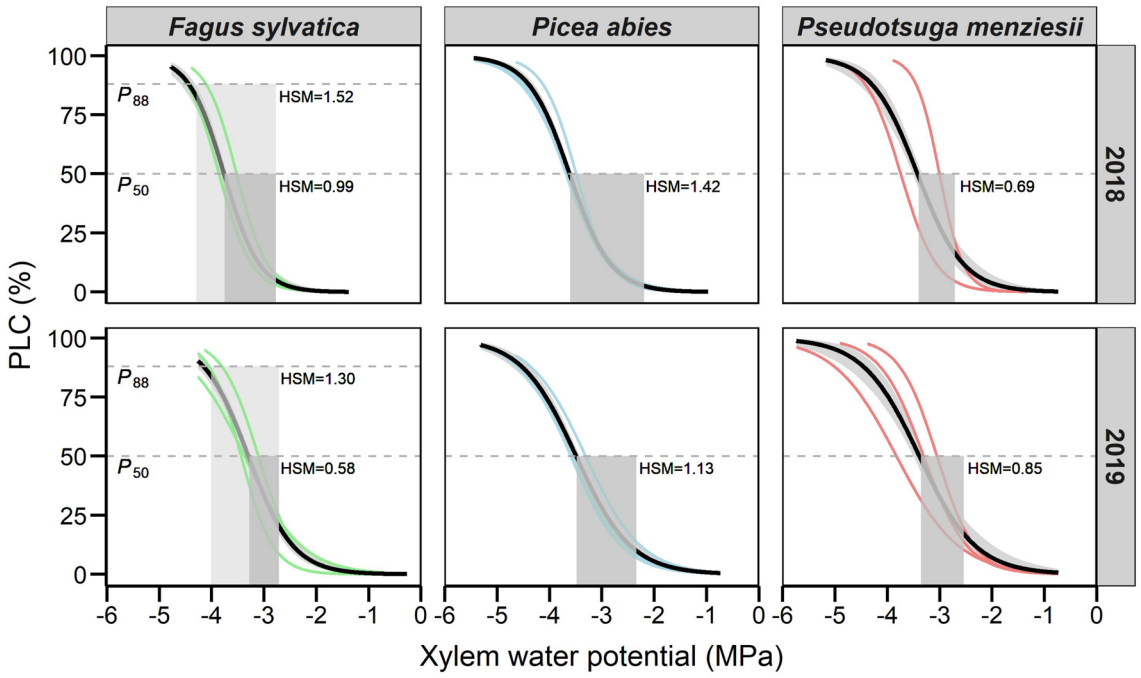

Fig. 6 Hydraulic safety margins (HSM) of *F. sylvatica, P. abies* and *P. menziesii* in the summers 2018 and 2019. Individual vulnerability curves for each tree are shown as percentage loss of conductivity (PLC, %) against xylem water potential (MPa) (mean of 3–4 samples each, colored lines) and at species level (black line). Shaded areas around VCs indicate 95% confidence interval of means. HSMs were calculated as lowest recorded Ψ_{Leaf}-values (Ψ_{min}) minus P_{50}-mean (average of all vulnerability curves of a species)

dry 2018 summer, *P. abies* showed g_S maxima of only 68 mmol m^{-2} s^{-1} and maintained very low midday stomatal conductance (g_{MD}) values throughout the summer (12.3 ± 11.1 mmol m^{-2} s^{-1}). Since our measurements began in 2018 in late June, it is possible that the conifers started the growing season with somewhat higher stomatal conductance, but reduced g_s rapidly at the onset of summer drought.

The relationship between g_S and Ψ_{Leaf} is often described by a positive sigmoid function (Klein 2014), when potential decreases lead to, or coincide with, a g_S reduction. Positive relations should be more clearly visible upon isohydric regulation, while strict anisohydric behavior may lead to negative relations, in which higher transpiration causes Ψ_{Leaf} to decrease, as has been reported for *F. sylvatica* (Leuschner et al. 2021). Our data show for the dry summers 2018 and 2019 in all three species not only positive, but also negative, diurnal $g_S - \Psi_{Leaf}$ relationships, hinting at complex interactions between turgor- and/or ABA-regulated feedback and VPD-driven feedforward regulation of g_S (McAdam et al. 2016; Franks et al. 2017). A dominant positive $g_S - \Psi_{Leaf}$ relationship appeared, when day-to-day changes during a drying cycle were considered, as expressed by the positive $g_{MD} - \Psi_{MD}$ relation. Over a few days to weeks, increasing drought intensity reduced both g_S and Ψ_{Leaf} in *F. sylvatica* as well as in *P. menziesii* (no relation appeared in *P. abies*).

Our stomatal conductance data produced no evidence for the assumption that *F. sylvatica* down-regulates g_S less sensitively in response to increasing VPD than *P. abies*, on the contrary. This questions a close association between isohydric behavior and stringent stomatal regulation (Martinez-Vilalta and Garcia-Forner 2017; Leuschner et al. 2021).

While the global data set of Choat et al. (2012) and other published data suggest that *P. menziesii* and *P. abies* should possess a more embolism-resistant branch xylem than *F. sylvatica*, this is not reflected in our data. The three species showed in both study years fairly similar P_{50}-values in the range of − 3.3 to − 3.8 MPa. The differences in P_{50} between *F. sylvatica* and *P. menziesii* were significant in 2018, despite considerable between-tree variation in the vulnerability curves of *P. menziesii* especially in 2019. Especially for *P. menziesii*, other studies have reported far more negative P_{50}-values than observed here (e.g., McCulloh et al. 2014: < − 5 MPa). Such contrasting outcomes of species comparisons are likely explained by considerable inter-population variation in the P_{50}-values of *P. menziesii* (Dalla-Salda et al. 2011, 2014; Eilmann et al. 2013), reflecting the wide climatic niche occupied by this species and high genetic

variation. The relatively high P_{50}-values of *P. menziesii* in our study might partly be a consequence of the relatively deep soils, which can buffer drought effects. In apparent contrast, inter-population variation in P_{50} of *F. sylvatica* has been found to be remarkably low, at least across climatic gradients in Central Europe (Wortemann et al. 2011; Schuldt et al. 2016; Weithmann et al. 2022b).

In our study, *F. sylvatica* and *P. menziesii* operated with relatively similar hydraulic safety margins (HSMs) of 0.6–1.0 MPa ($\Psi_{min} - P_{50}$), while the HSM of *P. abies* was larger (1.1 − 1.4 MPa). The similarity in HSMs of *F. sylvatica* and *P. menziesii* is surprising, given the assumed lower capacity of conifers for embolism repair (Johnson et al. 2012; Carnicer et al. 2013). Yet, after the 2018 drought, Arend et al. (2022) did not observe embolism repair in *F. sylvatica* trees suffering from impaired xylem function. In any case, it appears that adult *F. sylvatica* trees operate during mild to moderate drought with a HSM of at least 0.1 to 0.8 MPa in their sun-crown branches (Leuschner 2020 and references therein), while Dietrich et al. (2019) give an even higher value of 1.5 MPa. For *P. menziesii*, higher HSMs than observed here have also been reported (3 MPa, McCulloh et al. 2014). Our HSM data derived from the $\Psi_{min} - P_{50}$ difference in two extremely dry summers suggest a species ranking in the sequence *P. abies* > *F. sylvatica* ≈ *P. menziesii*, which changes to *F. sylvatica* > *P. abies* > *P. menziesii*, when the $\Psi_{min} - P_{88}$ difference is used in case of *F. sylvatica*. This contradicts the widespread assumption that conifers in general operate with wider branch xylem HSMs than angiosperm trees (Choat et al. 2012; Carnicer et al. 2013), disproving our second hypothesis. Due to the wide range of reported P_{50} and Ψ_{MD} values, it appears that hydraulic safety margins are year- and site-dependent. Studies covering a wide range of different environmental conditions would be needed to draw a more general conclusion about species differences in hydraulic safety.

In contrast to the remarkable similarity in branch hydraulic properties and also in the water potential at turgor loss point among the species, the conifers and *F. sylvatica* differed in the inter-annual variability of embolism resistance. We found only for *F. sylvatica* a marked shift of P_{12}, P_{50} and P_{88} from 2018 to 2019 by 0.3 − 0.6 MPa toward less negative potentials, while only little inter-annual change in branch hydraulic properties was recorded for the conifers. One possible explanation for decreased embolism resistance after the extreme 2018 drought is cavitation fatigue, likely caused by embolism-induced damage to conduit walls and pit membranes (Hacke et al. 2001; Christensen-Dalsgaard and Tyree 2013; Hillabrand et al. 2016), which has been observed in angiosperms, but seems to be rare in conifers including *P. abies* (Feng et al. 2021). Cavitation fatigue as a possible explanation for drought legacy effects has not yet been shown for *F. sylvatica*, but our results seem to indicate its existence.

P. abies maintained in both years a larger HSM than the other species, partly due to its stringent stomatal regulation. It closed its stomata in 2018 already 0.5 MPa above the P_{12} threshold, which agrees with results of other studies reporting a water-saving, cavitation-avoiding strategy in *P. abies* (Anfodillo et al. 1998; Lu et al. 1995; Sellin 2000). In our and some other studies, Ψ_{MD} did not drop below − 2.5 MPa (e.g., Lu et al. 1995; Cochard 1992), thus avoiding critical xylem tensions even in a drought as severe as in 2018. However, *P. abies* may well suffer catastrophic hydraulic failure, as was observed in summer 2018 in regions such as Switzerland, where cavitation triggered *P. abies* dieback in subsequent weeks (Schuldt et al. 2020; Arend et al. 2021). However, ψ_{min} reached − 4.2 MPa at this site, greatly surpassing the corresponding P_{12}-value (− 3.08 MPa), which contrasts with our results from the same year. Apparently, *P. abies* is drought-sensitive especially on shallow soils (Schmidt-Vogt 1977–1989; Modrzyński 2007; Lévesque et al. 2013), where the bulk of fine root biomass is restricted to the uppermost 20 or 30 cm of the profile. The deep sandy soils at our site, which allow somewhat deeper root penetration (Pietig et al., unpubl. data), might well explain the species' low vulnerability in this stand. Thus, *P. abies* may well be vulnerable to hydraulic failure and related dieback, despite its more isohydric behavior. This conclusion matches observations in a throughfall exclusion experiment in a mixed *F. sylvatica*-*P. abies* stand, where *P. abies* was more vulnerable to drought than *F. sylvatica* (Pretzsch et al. 2020; Grams et al. 2021).

Another important result is that HSMs were always positive in *P. abies* and *P. menziesii*, despite extreme drought in both summers, supporting the notion that stomatal closure normally prevents xylem pressure from traversing the steep section of the vulnerability curve (Meinzer et al. 2009). Yet, the negative $\Psi_{min} - P_{12}$ difference in *F. sylvatica* in summer 2019 indicates that emboli likely had formed at this instance in this species. Clearly, our results inform only about the species' response to the exceptional 2018/2019 drought, but do not reflect the behavior in climatically average years, which is better understood from the findings of other published studies.

Even though *P. menziesii* exhibited in 2018 an isohydric leaf water status regulation with the lowest g_S of all species, keeping stomata nearly closed throughout summer, the species operated with the smallest HSM close to its hydraulic limit. From the end of May onwards, the lower sun crown was hit by mealybug infestation (probably Douglas-fir mealybug, *Puto profusus*), and the needles discolored from mid of July onwards. This might have weakened the trees' defense due to impaired carbon assimilation and/or hydraulic failure. However, the *P. menziesii* trees did not suffer from

needle shedding or crown dieback in the subsequent months and years. *P. abies* and *F. sylvatica,* in contrast, were neither affected by widespread pathogen attack nor pre-senescent leaf/needle fall. However, *F. sylvatica* responded to the 2018 drought with the largest shift in leaf morphological and branch hydraulic traits, greatly decreasing leaf area and SLA and increasing Huber value in 2019, while reducing HSM. It is well established that *F. sylvatica* exhibits high plasticity in leaf morphological and/or hydraulic traits, which may increase drought acclimation (Schuldt et al. 2016; Weithmann et al. 2022a, b). In contrast, inter-annual trait variation was smaller in the conifers, probably in part due to the evergreen habitat. Constancy in morphological and anatomical traits was particularly striking in *P. menziesii*.

Conclusions

Our study during the exceptional 2018/2019 drought confirms the principally more anisohydric behavior of *F. sylvatica* and the more isohydric strategy of *P. abies* and *P. menziesii*. Nevertheless, our results contradict widely held assumptions of plant hydraulics, notably (1) the linkage of anisohydry to lose stomatal regulation (which is not the case in *F. sylvatica*), and (2) the existence of larger HSMs in conifers than in angiosperms (which is not true for *P. menziesii* at this site). Comparison with literature data indicates considerable spatial variation in the species' hydraulic safety margins, which can relate to edaphic and climatic gradients and genetic differences between populations, and may be due to the fact that our data reveal HSM minima, as they are encountered during extreme drought. Extrapolating our results from a sandy site to other edaphic conditions should be done only with great caution, as especially root system structure can differ between sites and populations. Rooting patterns and root physiology likely have a large and insufficiently understood influence on tree hydraulics and canopy water relations.

Our species comparison demonstrates that the 'conventional' analysis of branch xylem hydraulic safety, HSMs and stomatal regulation strategies is not sufficient for assessing the species' drought vulnerability at this sandy site. Moreover, we were not able to confirm the numerous literature reports about the high drought susceptibility of *P. abies*, nor the often-assumed higher drought resistance of *P. menziesii* (e.g., Vitali et al. 2017; Thomas et al. 2022). We conclude that a more comprehensive vulnerability assessment of these tree species has to consider additional traits such as rooting depth, shoot and root desiccation tolerance, the drought and heat sensitivity of photosynthesis and radial growth, evidence of drought-induced carbohydrate depletion, and the recovery potential after damage, among others.

Author contribution statement CL conceived the specific research idea, while CA conceived the interdisciplinary research group, CL and CA received the funding, KS conducted the field work and analyzed the data, MF collected part of the field data, CL and BS supervised the field work, and KS and CL wrote the paper. All authors commented on the text and approved it.

Supplementary Information The online version contains supplementary material available at https://doi.org/10.1007/s00468-024-02499-5.

Acknowledgements This research was conducted in the frame of Research Training Group GRK 2300 (project P2) with funding from the German Research Foundation (Deutsche Forschungsgemeinschaft). The financial support is gratefully acknowledged. We thank Heinz Coners for technical support throughout both study years and Mr. and Mrs. Gronau for providing us additional precipitation data and help during the field work.

Funding Open Access funding enabled and organized by Projekt DEAL. Deutsche Forschungsgemeinschaft, GRK 2300, Christoph Leuschner.

Data availability The data are available from the authors upon reasonable request.

Declarations

Conflict of interest The authors have no financial or non-financial interests to disclose.

References

Andrews SF, Flanagan LB, Sharp EJ, Cai T (2012) Variation in water potential, hydraulic characteristics and water source use in montane Douglas-fir and lodgepole pine trees in southwestern Alberta and consequences for seasonal changes in photosynthetic capacity. Tree Physiol 32:146–160

Anekonda TS, Lomas MC, Adams WT, Kavanagh KL, Aitken SN (2002) Genetic variation in drought hardiness of coastal Douglas-fir seedlings from British Columbia. Can J for Res 32:1701–1716

Anfodillo T, Rento S, Carraro C, Furlanetto L, Urbinati C, Carrer M (1998) Tree water relations and climatic variations at the alpine timberline: seasonal changes of sap flux and xylem water potential in Larix decidua Miller, *Picea abies* (L.) Karst. and *Pinus cembra* L. Ann For Sci 55:159–172

Arend M, Link R, Patthey R, Hoch G, Schuldt B, Kahmen A (2021) Rapid hydraulic collapse as cause of drought-induced mortality in conifers. PNAS 118:e2025251118

Arend M, Link RM, Zahnd C, Hoch G, Schuldt B, Kahmen A (2022) Lack of hydraulic recovery as a cause of post-drought foliage reduction and canopy decline in European beech. New Phytol. 234:1195–1205. https://doi.org/10.1111/nph.18065

Backes K, Leuschner C (2000) Leaf water relations of competitive *Fagus sylvatica* and *Quercus petraea* trees during 4 years differing in soil drought. Can J for Res 30:335–346

Bansal S, Harrington CA, Gould PJ, Bradley St. Clair J (2015) Climate-related genetic variation in drought-resistance of Douglas-fir (*Pseudotsuga menziesii*). Glob Change Biol 21:947–958

Bat-Enerel B, Weigel R, Leuschner C (2022) Changes in the thermal and hydrometeorological forest growth climate during 1948–2017 in northern Germany. Front For Glob Change 5:830977

Blackman CJ, Creek D, Maier C, Aspinwall MJ, Drake JE, Pfautsch S, O'Grady A, Delzon S, Medlyn BE, Tissue DT, Choat B (2019) Drought response strategies and hydraulic traits contribute to mechanistic understanding of plant dry-down to hydraulic failure. Tree Physiol 39:910–924

Bohn U, Neuhäusl R, Mitarbeit U (2003) Map of the natural vegetation of Europe Scale 1:2500000. Bundesamt für Naturschutz (BfN)/ Federal Agency for Nature Conservation, Bonn

Braun S, Hopf S-E, Tresch S, Remund J, Schindler C (2021) 37 Years of forest monitoring in Switzerland: drought effects on *Fagus sylvatica*. Front For Glob Change 4:765782

Brix H, Mitchell AK (1986) Thinning and nitrogen fertilization effects on soil and tree water stress in a Douglas-fir stand. Can J for Res 16:1334–1338

Büntgen U, Urban O, Krusic PJ et al (2021) Recent European drought extremes beyond Common Era background variability. Nat Geosci 14:190–196

Carnicer J, Barbeta A, Sperlich D, Coll M, Penuelas J (2013) Contrasting trait syndromes in angiosperms and conifers are associated with different responses of tree growth to temperature on a large scale. Front Plant Sci 4:409

Choat B, Jansen S, Brodribb TJ, Cochard H, Delzon S, Bhaskar R et al (2012) Global convergence in the vulnerability of forests to drought. Nature 491:752–755

Christensen-Dalsgaard KK, Tyree MT (2013) Does freezing and dynamic flexing of frozen branches impact the cavitation resistance of *Malus domestica* and the *Populus* clone Walker? Oecologia 3:665–674

Cochard H (1992) Vulnerability of several conifers to air embolism. Tree Physiol 11:73–83

Cochard H, Damour G, Bodet C, Tharwat I, Poirier M, Améglio T (2005) Evaluation of a new centrifuge technique for rapid generation of xylem vulnerability curves. Physiol Plant 124:410–418

Cocozza C, de Miguel M, Pšidová E, Ditmarová L, Marino S, Maiuro L, Alvino A, Czajkowski T, Bolte A, Tognetti R (2016) Variation in ecophysiological traits and drought tolerance of beech (*Fagus sylvatica* L.) seedlings from different populations. Front Plant Sci 7:886

Dalla-Salda G, Martinez-Meier A, Cochard H, Rozenberg P (2011) Genetic variation of xylem hydraulic properties shows that wood density is involved in adaptation to drought in Douglas-fir (*Pseudotsuga menziesii* (Mirb.)). Ann For Sci 68:747–757

Dalla-Salda G, Fernández ME, Sergent AS, Rozenberg P, Badel E, Martinez-Meier A (2014) Dynamics of cavitation in a Douglas-fir tree-ring: transition-wood, the lord of the ring? J Plant Hydraul 1:e-0005

Delzon S, Douthe C, Sala A, Cochard H (2010) Mechanism of water-stress induced cavitation in conifers: bordered pit structure and function support the hypothesis of seal capillary-seeding. Plant Cell Environ 33:2101–2111

Dietrich L, Delzon S, Hoch G, Kahmen A (2019) No role for xylem embolism or carbohydrate shortage in temperate trees during the severe 2015 drought. J Ecol 107:334–349

Domec J-C, Gartner BL (2001) Cavitation and water storage capacity in bole xylem segments of mature and young Douglas-fir trees. Trees 15:204–214

Eilmann B, de Vries SM, den Ouden J, Mohren GM, Sauren P, Sass-Klaassen U (2013) Origin matters! Difference in drought tolerance and productivity of coastal Douglas-fir (*Pseudotsuga menziesii* (Mirb.)) provenances. For Ecol Manag 302:133–143

Feng F, Losso A, Tyree M, Zhang S, Mayr S (2021) Cavitation fatigue in conifers: a study on eight European species. Plant Physiol 186:1580–1590

Fischer EM, Schär C (2008) Future changes in daily summer temperature variability: driving processes and role for temperature extremes. Clim Dyn 33:917–935

Franks PJ, Berry JA, Lombardozzi DL, Bonan GB (2017) Stomatal function across spatial and temporal scales: deep-time trends, land-atmosphere coupling and global models. Plant Physiol 174:583–602

Frei ER, Gossner MM, Vitasse Y, Queloz V, Dubach V, Gessler A, Ginzler C, Hagedorn F, Meusberger K et al (2022) European beech dieback after premature leaf senescence during the 2018 drought in northern Switzerland. Plant Biol 24:2231–1145

Gessler A, Keitel C, Nahm M, Rennenberg H (2004) Water shortage affects the water and nitrogen balance in Central European beech forests. Plant Biol 6:289–298

Goisser M, Geppert U, Rötzer T, Paya A, Huber A, Kerner R et al (2016) Does belowground interaction with *Fagus sylvatica* increase drought susceptibility of photosynthesis and stem growth in Picea abies? For Ecol Manag 375:268–278

Grams TE, Hesse BD, Gebhardt T, Weikl F, Rötzer T, Kovacs B, Hikino K, Hafner BD, Brunn M, Bauerle T, Häberle K-H, Pretzsch H, Pritsch K (2021) The Kroof experiment: realization and efficacy of a recurrent drought experiment plus recovery in a beech/spruce forest. Ecosphere 12:e03399

Hacke U, Sauter J (1995) Vulnerability of xylem to embolism in relation to leaf water potential and stomatal conductance in *Fagus sylvatica* f. purpurea and Populus balsamifera. J Exp Bot 46:1177–1183

Hacke UG, Stiller V, Sperry JS, Pittermann J, McCulloh A (2001) Cavitation fatigue. Embolism and refilling cycles can weaken the cavitation resistance of xylem. Plant Physiol 125:779–786

Hajek P, Leuschner C, Hertel D, Delzon S, Schuldt B (2014) Trade-offs between xylem hydraulic properties, wood anatomy and yield in *Populus*. Tree Physiol 34:744–756

Hartmann H, Ziegler W, Kolle O, Trumbore S (2013) Thirst beats hunger–declining hydration during drought prevents carbon starvation in Norway spruce saplings. New Phytol 200:340–349

Hillabrand RM, Hacke UG, Lieffers VJ (2016) Drought-induced xylem pit membrane damage in aspen and balsam poplar. Plant Cell Environ 10:2210–2220

Jansen K (2017) Stable isotopes and metabolite profiles as physiological markers for the drought stress sensitivity in Douglas fir provenances (*Pseudodtsuga menziesii* (Mirb.) Franco). Ph.D. Thesis. Humboldt University, Berlin

Johnson DM, McCulloh KA, Woodruff DR, Meinzer FC (2012) Hydraulic safety margins and embolism reversal in stems and leaves: why are conifers and angiosperms so different? Plant Sci 195:48–53

Kahmen A, Basler D, Hoch G, Link RM, Schuldt B, Zahnd C, Arend M (2022) Root water uptake depth determines the hydraulic vulnerability of temperate European tree species during the extreme 2018 drought. Plant Biol 4:1–2

Keller T, Wehrmann J (1963) CO_2-Assimilation, Wurzelatmung und Ertrag von Fichten- und Kiefernsämlingen bei unterschiedlicher Mineralstoffernährung. Mitt. Schweiz Anstalt Für Das Forstliche Versuchswesen 39:217–242

Kerhoulas L, Polda W, Kerhoulas N, Berrill J-P (2020) Physiology and growth of Douglas-fir and redwood seedlings planted after partial harvesting. Front For Glob Change 3:49

Klein T (2014) The variability of stomatal sensitivity to leaf water potential across tree species indicates a continuum between isohydric and anisohydric behaviours. Funct Ecol 6:1313–1320

Köcher P, Gebauer T, Horna V, Leuschner C (2009) Leaf water status and stem xylem flux in relation to soil drought in five temperate broad-leaved tree species with contrasting water use strategies. Ann For Sci 66:101–111

Koide RT, Robichaux RH, Morse RH, Smith CM (2000) Plant water status, hydraulic resistance and capacitance. In: Pearcy RW, Ehleringer JR, Mooney HA, Rundel PW (eds) Plant physiological ecology: field methods and instrumentation. Kluwer, Dordrecht, pp 161–183

Krejza J, Cienciala E, Svetlik J, Bellan M, Noyer E, Horacek P, Stepanek P, Marek MV (2021) Evidence of climate-induced stress of Norway spruce along elevation gradient preceding the current dieback in Central Europe. Trees 35:103–119

Leo M, Oberhuber W, Schuster R, Grams TEE, Matyssek R, Wieser G (2014) Evaluating the effect of plant water availability on inner alpine coniferous trees based on sap flow measurements. Eur J For Res 133:691–698

Leuschner C (2020) Drought response of European beech (*Fagus sylvatica* L.)—a review. Perspect Plant Ecol Evol Syst 47:125576

Leuschner C, Ellenberg H (2017) Ecology of central European forests. Vegetation ecology of central Europe, vol I. Springer Nature, Cham

Leuschner C, Wedde P, Lübbe T (2019) The relation between pressure-volume curve traits and stomatal regulation of water potential in five temperate broadleaf tree species. Ann For Sci 76:60

Leuschner C, Schipka F, Backes K (2021) Stomatal regulation and water potential variation in European beech: challenging the iso/anisohydry concept. Tree Physiol 42:365–378

Leuschner C, Weithmann G, Bat-Enerel B, Weigel R (2023) The future of European beech in Northern Germany—climate change vulnerability and adaptation potential. Forests 14:1448

Lévesque M, Saurer M, Siegwolf R, Eilmann B, Brang P, Bugmann H, Rigling A (2013) Drought response of five conifer species under contrasting water availability suggests high vulnerability of Norway spruce and European larch. Glob Change Biol 19:3184–3199

Link P, Simonin K, Maness H, Oshun J, Dawson T, Fung I (2014) Species differences in the seasonality of evergreen tree transpiration in a Mediterranean climate: analysis of multiyear, half-hourly sap flow observations. Water Resour Res 50:1869–1894

Lobo A, Torres-Ruiz JM, Burlett R, Lemaire C, Parise C, Francioni C, Truffaur L, Tomaskova I, Hansen JK, Kjaer ED, Kremer A, Delzon S (2017) Assessing inter- and intraspecific variability of xylem vulnerability to embolism in oaks. For Ecol Manag 424:53–61

Lu P, Biron P, Granier A, Cochard H (1995) Water relations of adult Norway spruce (*Picea abies* (L) Karst) under soil drought in the Vosges mountains: whole-tree hydraulic conductance, xylem embolism and water loss regulation. Ann For Sci 53:113–121

Lübbe T, Lamarque LJ, Delzon S, Ruiz JMT, Burlett R, Leuschner C, Schuldt B (2022) High variation in hydraulic efficiency but not xylem safety between roots and branches in four temperate broad-leaved tree species. Funct Ecol 36:699–712

Lyr H, Fiedler HJ, Tranquillini W (1992) Physiologie und Ökologie der Gehölze. G. Fischer, Jena

Maherali H, Pockman WT, Jackson RB (2004) Adaptive variation in the vulnerability of woody plants to xylem cavitation. Ecology 85:2184–2199

Martinez-Sancho E, Vasconez Navas LK, Seidel H, Dorado-Linan I, Menzel A (2017) Responses of contrasting tree functional types to air warming and drought. Forests 8:450

Martinez-Vilalta J, Garcia-Forner N (2017) Water potential regulation, stomatal behaviour and hydraulic transport under drought: deconstructing the iso/anisohydric concept. Plant Cell Environ 40:962–976

McAdam SAM, Sussmilch FC, Brodribb TJ (2016) Stomatal responses to vapour pressure deficit are regulated by high speed gene expression in angiosperms. Plant Cell Environ 39:485–491

McCulloh KA, Johnson DM, Meinzer FC, Woodruff D (2014) The dynamic pipeline: hydraulic capacitance and xylem hydraulic safety in four tall conifer species. Plant Cell Environ 5:1171–1183

McDowell N, Pockman WT, Allen CD, Breshears DD, Cobb N, Kolb T et al (2008) Mechanisms of plant survival and mortality during drought: why do some plants survive while others succumb to drought? New Phytol 178:719–739

Meinke I, Gerstner E, von Storch H, Marx A, Schipper H, Kottmeier C, Treffeisen R, Lemke P (2010) Regionaler Klimaatlas Deutschland der Helmholtz-Gemeinschaft informiert im Internet über möglichen künftigen Klimawandel. DMG Mitteilungen 2:7–9

Meinzer FC, Johnson DM, Lachenbruch B, McCulloh KA, Woodruff DR (2009) Xylem hydraulic safety margins in woody plants: coordination of stomatal control of xylem tension with hydraulic capacitance. Funct Ecol 23:922–930

Modrzyński J (2007) Outline of ecology. In: Tjoelker MG, Boratyński A, Bugała W (eds) Biology and ecology of Norway spruce forestry sciences, vol 78. Springer, Dordrecht. https://doi.org/10.1007/978-1-4020-4841-8_11

Niinemets U, Valladares F (2006) Tolerance to shade, drought, and waterlogging of temperate Northern Hemisphere trees and shrubs. Ecol Monogr 76:521–547

Oberhuber W, Hammerle A, Kofler W (2015) Tree water status and growth of saplings and mature Norway spruce (*Picea abies*) at a dry distribution limit. Front Plant Sci 6:703

Obladen N, Dechering P, Skiaderesis G, Tegel W, Keßler J, Höllerl S, Kaps S, Hertel M, Choimaa D, Seifert T, Hirsch M, Seim A (2021) Tree mortality of European beech and Norway spruce induced by 2018–2019 hot droughts in Central Germany. Agric For Meteorol 307:108482

Pammenter NW, Vander Willigen C (1998) A mathematical and statistical analysis of the curves illustrating vulnerability of xylem to cavitation. Tree Physiol 18:589–593

Perterer J, Körner C (1990) Das Problem der Bezugsgröße bei physiologisch-ökologischen Untersuchungen an Koniferennadeln. Forstwiss Centralblatt 109:220–241

Phillips N, BaJ B, McDowell NG, Ryan MG (2002) Canopy and hydraulic conductance in young, mature and old Douglas-fir trees. Tree Physiol 22:205–211

Piñol J, Sala A (2000) Ecological implications of xylem cavitation for several Pinaceae in the Pacific Northern USA. Funct Ecol 14:538–545

Pretzsch H, Grams T, Häberle K-H, Pritsch K, Bauerle T, Rötzer T (2020) Growth and mortality of Norway spruce and European beech in monospecific and mixed-species stands under natural episodic and experimentally extended drought. Results of the KROOF throughfall exclusion experiment. Trees 34:957–970

Prometheuswiki (2018) Leaf pressure-volume curve parameters. https://prometheuswiki.rsb.anu.edu.au/tiki-index.php?page=Pressure-volume+curves. Accessed 9 2021

R Core Team (2013) R: a language and environment for statistical computing. Vienna, Austria. https://www.Rproject.org/. version 4.0.5
Running SW (1976) Environmental control of leaf water conductance in conifers. Can J for Res 6:104–112
Schuldt B, Knutzen F, Delzon S, Jansen S, Müller-Haubold H, Burlett R, Clough Y, Leuschner C (2016) How adaptable is the hydraulic system of European beeach in the face of climate change-related precipitation reduction. New Phytol 210:443–548
Schuldt B, Buras A, Arend M, Vitasse Y, Beierkuhnlein C, Damm A et al (2020) A first assessment of the impact of the extreme 2018 summer drought on Central European forests. Basic Appl Ecol 45:86–103
Schulze E-D, Fuchs MI, Fuchs M (1977) Spacial distribution of photosynthetic capacity and performance in a mountain spruce forest of northern Germany. Oecologia 29:43–61
Sellin A (2000) Hydraulic and stomatal adjustment of Norway spruce trees to environmental stress. Tree Physiol 21:879–888
Senf C, Buras A, Zang CS, Rammig A, Seidl R (2020) Excess forest mortality is consistently linked to drought across Europe. Nat Commun 11:6200
Sokal RR, Rohlf FJ (1995) Biometry. The principles and practice of statistics in biological research, 3rd edn. W. H. Freeman and Co, New York
Sperry JS, Ikeda T (1997) Xylem cavitation in roots and stems of Douglas-fir and white fir. Tree Physiol 17:275–280
Spiecker H, Lindner M, Schuler J (2019) (eds) Douglas-fir—an option for Europe. European Forest Institute, Joensuu
Spinoni J, Vogt JV, Naumann G, Barbosa P, Dosio A (2018) Will drought events become more frequent and severe in Europe? Int J Climatol 38:1718–1736
Stinziano JR, Hüner NPA, Way DA (2015) Warming delays autumn declines in photosynthetic capacity in a boreal conifer, Norway spruce (*Picea abies*). Tree Physiol 35:1303–1313
Thomas F, Rzepecki A, Werner W (2022) Non-native Douglas fir (*Pseudotsuga menziesii*) in Central Europe: ecology, performance and nature conservation. For Ecol Manag 506:119956
Thonfeld F, Gessner U, Holzwarth S, Kriese J, da Ponte E, Huth J, Kuenzer C (2022) A first assessment of canopy cover loss in Germany's forests after the 2018–2020 drought years. Remote Sens 14:562
Thünen Institute (2015) Dritte Bundeswaldinventur—Basisdaten. https://bwi.info/inhalt1.3.aspx?Text=1.04%20Baumartengruppe%20(rechnerischer%20Reinbestand)&prrolle=public&prInv=BWI2012&prKapitel=1.04&mpXicode=. Accessed 7 Mar 2022
Tomasella M, Beikircher B, Häberle K-H, Hesse B, Kallenbach C, Matyssek R, Mayr S (2017) Acclimation of branch and leaf hydraulics in adult *Fagus sylvatica* and *Picea abies* in a forest through-fall exclusion experiment. Tree Physiol 38:198–211
Trnka M, Hlavinka P, Semenov MA (2015) Adaptation options for wheat in Europe will be limited by increased adverse weather events under climate change. J R Soc Interface 12:20150721
Tumajer J, Altman J, Stepanek P, Treml V, Dollezal J, Cienciala E (2017) Increasing moisture limitation of Norway spruce in Central Europe revealed by forward modelling of tree growth in tree-ring network. Agric For Meteorol 247:56–64
Tyree MT, Jarvis PG (1982) Water in tissues and cells. Encyclopedia plant physiol N.S., vol 12B. Springer, Berlin, pp 35–77
Tyree MT, Zimmermann MH (2002) Xylem structure and the ascent of sap, 2nd edn. Springer, Berlin
Urli M, Porté AJ, Cochard H, Guengant Y, Burlett R, Delzon S (2013) Xylem embolism threshold for catastrophic hydraulic failure in angiosperm trees. Tree Physiol 33:672–683
Vitali V, Büntgen U, Bauhus J (2017) Silver fir and Douglas fir are more tolerant to extreme droughts than Norway spruce in south-western Germany. Glob Chang Biol 23:5108–5119
Voelker SL, deRose RJ, Bekker MF, Sriladda C, Leksungnoen N, Kjelgren RK (2018) Anisohydric water use behavior links growing season evaporative demand to ring-width increment in conifers from summer-dry environments. Trees 32:735–749
Wallin G, Skärby L, Selldén G (1990) Long-term exposure of Norway spruce, *Picea abies* (L.) Karst., to ozone in open-top chambers. New Phytol 115:335–344
Walthert L, Ganthaler A, Mayr S, Saurer M, Waldner P, Walser M et al (2021) From the comfort zone to crown dieback: sequence of physiological stress thresholds in mature European beech trees across progressive drought. Sci Total Environ 753:141792
Warren CR, Livingston NJ, Turpin DH (2003) Responses of gas exchange to reversible changes in whole-plant transpiration rate in two conifer species. Tree Physiol 23:793–803
Warren CR, Livingston NJ, Turpin DH (2004a) Water stress decreases the transfer conductance of Douglas-fir (*Pseudotsuga menziesii*) seedlings. Tree Physiol 24:971–979
Weithmann G, Schuldt B, Link RM, Heil D, Hoeber S, John H, Müller-Haubold H, Schumann K, Leuschner C (2022a) Leaf trait modification in European beech trees in response to climatic and edaphic drought. Plant Biol 24:1272–1286
Weithmann G, Link RM, Banzragch B-E, Würzberg L, Leuschner C, Schuldt B (2022b) Soil water availability and branch age explain variability in xylem safety of European beech in Central Europe. Oecologia 198:629–644
Williams AP, Allen CD, Macalady AK, Griffin D, Woodhouse CA, Meko DM, Swetnam TW, Rauscher SA, Seager R, Grissino-Mayer HD et al (2013) Temperature as a potent driver of regional forest drought stress and tree mortality. Nat Clim Chang 3:292–297
Wortemann R, Herbette S, Barigah TS, Fumanal B, Ducousso A, Gömöry D, Roeckel-Drevet P, Cochard H (2011) Genotypic variability and phenotypic plasticity of cavitation resistence in *Fagus sylvatica* L. across Europe. Tree Physiol 31:1175–1182
Zeller B, Legout A, Bienaimé S, Gratia B, Santenoise P, Bonnaud P, Ranger J (2019) Douglas fir stimulates nitrification in French forest soils. Sci Rep 9:1–11
Zweifel R, Steppe K, Sterck FJ (2007) Stomatal regulation by microclimate and tree water relations: interpreting ecophysiological field data with a hydraulic plant model. J Exp Bot 58:2113–2131
Zweifel R, Rigling A, Dobbertin M (2009) Species-specific stomatal response of trees to drought—a link to vegetation dynamics? J Veg Sci 20:442–454